

# cETX: Incorporating Spatiotemporal Correlation for Better Wireless Networking

Song Min Kim   Shuai Wang   Tian He

Department of Computer Science and Engineering  
University of Minnesota

{ksong, shuaiw, tianhe}@cs.umn.edu

## ABSTRACT

In this work, we experimentally observe the existence of spatiotemporal correlation among adjacent wireless links within short time intervals. Such an observation calls attention to potential errors in existing popular metrics built upon the assumption of link independence. Specifically we propose cETX (correlated ETX), a generalized metric, to compensate for estimation errors suffered by the widely-adopted ETX in the presence of correlated interference. To the best of our knowledge, this is the first work to introduce a unified metric embracing both temporal and spatiotemporal correlations. The highlight of the cETX metric is its broad applicability and effectiveness. Evaluations on ZigBee (802.15.4) and Wi-Fi (802.11b/g/n) testbeds deployed in a lab, corridor, and on a bridge reveal that: Simply replacing ETX with cETX (i) cuts down the error by 70.2% and 62.1%, respectively, and (ii) saves averages of 22% and 37% communication cost in three unicast [4, 13, 17] and nine broadcast protocols [7, 18, 23, 24, 27, 30, 40] at the price of only 0.7% additional overhead.

## Categories and Subject Descriptors

C.2.1 [Network Architecture and Design]: Wireless communications

## Keywords

Wireless routing; Route metrics; Energy efficiency

## 1. INTRODUCTION

Wireless links are unreliable and prone to losses due to noise and interference [16, 19, 35, 36, 42]. To effectively utilize these unreliable wireless links, research calls for metrics that can accurately estimate the qualities of individual links as well as end-to-end paths. Among the extensive volume of admirable studies dealing with routing under lossy links [8, 11, 41], expected transmission count (ETX) [11] is the most popular for its generality and effectiveness, and has been cited over 3,000 times according to Google Scholar.

Permission to make digital or hard copies of all or part of this work for personal or classroom use is granted without fee provided that copies are not made or distributed for profit or commercial advantage and that copies bear this notice and the full citation on the first page. Copyrights for components of this work owned by others than ACM must be honored. Abstracting with credit is permitted. To copy otherwise, or republish, to post on servers or to redistribute to lists, requires prior specific permission and/or a fee. Request permissions from [Permissions@acm.org](mailto:Permissions@acm.org).

*SensSys '15*, November 1–4, 2015, Seoul, South Korea.

© 2015 ACM. ISBN 978-1-4503-3631-4/15/11 ...\$15.00.

DOI: <http://dx.doi.org/10.1145/2809695.2809704>.

Our further studies on link characteristics, however, reveal that ETX suffers from a few limitations. First, recent work on the temporal property of wireless links [10, 32] shows that transmissions over a link within a short time interval are highly dependent, indicating the existence of temporal correlation among transmissions. This property is not taken into account in the design of the ETX metric, imposing a limitation on its ability to reflect the true link quality. This is because ETX is defined as the inverse of packet reception ratio (PRR). This value is in fact the mean of the geometric random variable with independent trials, indicating that ETX is implicitly built on the independence assumption among transmissions.

Another link characteristic enlightened by current work ([28, 33]) is the existence of a reception correlation among the receivers of broadcast packets due to cross-network interference and correlated shadowing. Simply put, the receptions of broadcast packets at adjacent nodes are correlated at the same time instant, indicating spatial correlation. In this work, we observe that spatial correlation interplays with temporal correlation to exhibit reception correlation at consecutive links. In other words, there exists spatiotemporal correlation, i.e., the packet reception of a link is dependent on the recent reception at preceding links along a path. Since existing metrics including ETX are hop-by-hop designs, they fail to take spatiotemporal correlation into account.

In this paper, we reveal why ETX cannot represent the true quality of links in the face of temporal and spatiotemporal correlation. To address this issue, we design an enhanced version of ETX, called correlated ETX (cETX) that explores the phenomena to reflect the true performance of links and paths more precisely compared to ETX. In detail, we provide a unified metric embracing both temporal and spatiotemporal correlation factors. While keeping the intuitive idea of ETX intact (i.e., explicitly quantifying expected number of transmissions), our metric selects better links and paths that leads to less transmissions, thus achieving energy savings. In summary, our contributions are as follows:

- We experimentally reveal the phenomenon of spatiotemporal correlation and its potential impact on routing designs.
- We propose a new metric – cETX, capable of capturing temporal and spatiotemporal properties of wireless links. To the best of our knowledge, this is the first work to embed the two effects into a unified metric.
- We demonstrate how to incorporate cETX into (i) classical shortest path unicast algorithms and (ii) clas-

sical/collaborative broadcast algorithms, while maintaining the unicast path optimality and minimizing network-wide broadcast overhead distributively.

- We compare the accuracy of cETX and ETX through ZigBee and Wi-Fi testbed experiments, and via analysis on the Roofnet [3] trace to demonstrate error reduction of 70.2%, 62.1%, and 33.2%, respectively.
- We experimentally validate the applicability and effectiveness of cETX by replacing ETX with cETX in three unicast and nine broadcast protocols utilizing diverse network structures. cETX cuts down averages of 22% and 37% communication cost at the price of only 0.7% additional overhead via parameter piggybacking.

The paper is organized as follows. Section 2 motivates the work. Section 3 follows with the underlying model and reasoning. Section 4 and Section 5 present the design and implementation of cETX, where its applications are introduced in Section 6. Section 7 evaluates cETX, followed by in-situ deployment demonstration in Section 8. We summarize related work in Section 9 and conclude in Section 10.

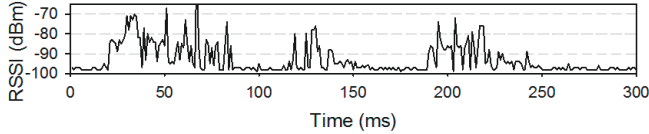


Figure 1: Interference Burst

## 2. MOTIVATION

Spatiotemporal correlation occurs with the interference and shadowing spanning through multiple links and last for a duration of multiple packets. Figure 1 shows the interference captured under an office environment where many of the spike bursts last over tens of milliseconds. The captured signal strength ranges from -70 to -90dBm, a level of typical Wi-Fi signals. In sum, the observed interference from Wi-Fi is not only explosive, but also strong enough to simultaneously affect multiple low-power 802.15.4 links, suggesting that it is one of the causes of spatiotemporal correlation.

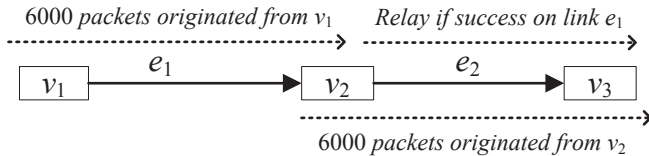


Figure 2: Experiment Topology

### 2.1 Spatiotemporal Correlation Revealed

We experimentally validate the phenomenon of spatiotemporal correlation in practice, among consecutive wireless links along a path. A simple two-hop network is formed as shown in Figure 2, operating on 802.15.4 channel 12 with a transmission power of -25dBm. Ten such networks are deployed for statistical significance. In each network, two cases are tested. **Case #1:** Node  $v_1$  transmits 6000 packets to  $v_2$ . Upon successfully receiving a packet,  $v_2$  relays the packet to  $v_3$  five times, each after 2, 8, 14, 20, and 26ms delay. **Case #2:** Node  $v_2$  transmits 6000 packets generated by itself to  $v_3$ . Please note that, in case #1, transmission over link  $e_2$

only occurs upon success on  $e_1$ . Therefore the reception success probability on  $e_2$  in this case is conditional, given the success on preceding link  $e_1$ . On the other hand, the success probability over  $e_2$  in case #2 is considered marginal, as it is irrelevant to  $e_1$ .

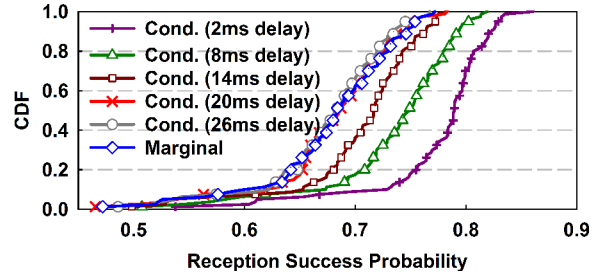


Figure 3: Validating spatiotemporal correlation: whenever  $v_2$  successfully receives a packet from  $v_1$  it relays the packet five times to  $v_3$  with different delays after reception. Thus, the success ratio of the relayed packets are *conditional* to the success of the transmission from  $v_1$  to  $v_2$ , whereas the packets originated at  $v_2$  are *marginal*.

Figure 3 shows the experiment results of  $e_2$ 's reception success probabilities, where conditional curves are obtained from case #1, and the marginal is from case #2. There exists a significant difference between the conditional probability with 2ms delay and the marginal probability. This supports the existence of spatiotemporal (positive) correlation between  $e_1$  and  $e_2$ . That is, success on the preceding link ( $e_1$ ) strongly implies success on the following link ( $e_2$ ). Moreover, 20 and 26ms curves nearly overlap with the marginal curve, indicating spatiotemporal correlation fades away after 20ms. To conclude, the experiment result gives us a simple but effective design guidance: We can increase the chance of a successful reception of a packet by simply relaying it within a short time interval, e.g., within 20ms in our experiment.

Link1:	F	S	S	F	S	F	F	S	F	S
Link2:	F	F	F	S	S	S	F	F	S	S
	$t_0$	$t_1$	$t_2$	$t_3$	$t_4$	$t_5$	$t_6$	$t_7$	$t_8$	$t_9$

Figure 4: Temporal correlation effect: Despite the same reception ratios, bursty failure in Link2 demands 1.9 transmissions where Link1 requires 1.6.

### 2.2 Impact of Temporal Correlation

We illustrate the effect of temporal correlation via a simple example in Figure 4. In the history of ten transmissions of two links,  $S$  and  $F$  represent transmission success and failure. Since both links experience five  $S$  and five  $F$ , ETX indicates that the two links have equal performance, i.e.,  $10/5=2$  expected transmissions. However, the true average transmissions are not equal. Let's consider the case where we start transmitting at  $t_0$ . On Link1, the transmission succeeds at  $t_1$  which causes two transmissions (i.e., fail at  $t_0$ , success at  $t_1$ ). It costs four on Link2 as it succeeds at  $t_3$  after three failures. Similarly, when we start the transmission at  $t_1$ , Link1 succeeds in a single transmission, while Link2 requires three.

When the start of a transmission occurs with equal probabilities across  $t_0 - t_9$ , we obtain the true average number of

transmissions by repeating the above process up to  $t_9$  and taking the average. This yields  $(2 + 1 + \dots + 1)/10 = 1.6$  and  $(4 + 3 + \dots + 1)/10 = 1.9$  for Link1 and Link2, indicating that Link1 is indeed a better link, despite their equal ETX. The performance difference of the two links can be described via conditional probability of failure followed by success, i.e.,  $Pr(S^n|F^{n-1})$  for  $1 \leq n \leq 9$ . This represents the link's ability to recover from failures. Thus, larger value indicate better performance. The values are 0.8 and 0.4 for Link1 and Link2, which confirms our argument.



**Figure 5: Temporal Correlation in real trace forces two links with similar reception ratios to exhibit different demands of 2.05 and 2.98 transmissions.**

The observation is further verified on the real traces in Figure 5, collected from two pairs of MICAz nodes. Each trace from two links holds a record of  $10^3$  packet transmissions. Black bars indicate failures while whites indicate successes. The packet reception ratios of Link3 and Link4 are 0.49 and 0.5, leading to approximately the same ETX of 2 for both links. However, the difference in the true average transmissions is quite large; 2.05 and 2.98 for Link3 and Link4, respectively. This is due to the consecutive failure chunks demonstrated in Link4; it is less able to recover from the failure than Link3. This difference again can be represented by the conditional probability. The values of  $Pr(S^n|F^{n-1})$  are 0.49 and 0.29 for Link3 and Link4.

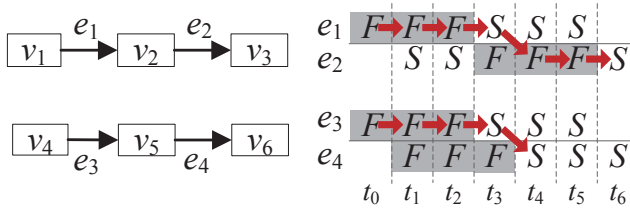


**Figure 6: Higher spatiotemporal correlation in consecutive links allows a better chance of success on the succeeding link following the link preceding it. Marked with arrows, the number of transmissions for an end-to-end delivery is therefore smaller for the lower path.**

### 2.3 Impact of Spatiotemporal Correlation

In Figure 6, we use two two-hop paths to show how spatiotemporal correlation affects the network performance that ETX fails to capture. The packet reception ratios of every link in the figure,  $e_1$ - $e_4$ , are equally  $1/2$ . This yields ETX value of  $2 + 2 = 4$  for both upper and lower paths. However, the links in the lower path,  $e_3$  and  $e_4$ , are more positively correlated to each other than those ( $e_1$  and  $e_2$ ) in the upper path. Starting with the upper path, suppose that node  $v_1$  has a packet to deliver to node  $v_3$  and starts sending at time  $t_0$ . The packet successfully reaches  $v_2$  after four transmissions (i.e.  $F \rightarrow F \rightarrow F \rightarrow S$ ). The transmission on

$e_2$  starts at  $t_4$  but succeeds at  $t_6$ , consuming three transmissions ( $F \rightarrow F \rightarrow S$ ). Therefore, end-to-end delivery in the upper path consumes a total of seven transmissions. This forwarding flow is demonstrated in Figure 6 as arrows. Similarly, we can easily see that the lower path requires five transmissions. This indicates that the lower path performs better than the upper path, despite their equivalence in the ETX values.

This example suggests that spatiotemporal correlation can improve the network performance. That is, when consecutive links in a path are strongly (positively) correlated, forwarding a packet shortly after receiving it from the preceding link has a high chance of successful receptions in the following link. Therefore, spatiotemporal correlation should be considered for an accurate performance measurement in multi-hop scenarios. To do so, we represent the degree of spatiotemporal correlation with conditional probability, i.e.,  $Pr(S_i^n|S_{i-1}^{n-1})$  at arbitrary time  $t_n$  when  $e_{i-1}$  precedes  $e_i$ . To verify, the conditional probability in this example yields  $0.33 = Pr(S_2^n|S_1^{n-1}) < Pr(S_4^n|S_3^{n-1}) = 1$ , correctly reflecting the relative performance of the two paths under spatiotemporal correlation.

## 3. DESIGN BACKGROUND

In this section, we first present the model that lays the foundation of our design. Then, we provide empirical evidences and analysis on the suitability of such a model for our purpose of capturing correlation.

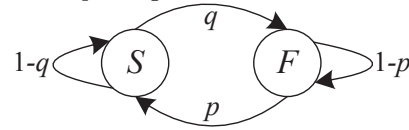


**Figure 7: Gilbert Model**

### 3.1 Underlying Model

This section presents the underlying model to help understand our design presented in the next section. Recall in section 2 we showed that both temporal and spatiotemporal correlations can be quantified by conditional probabilities. A simple way of modeling with conditional probabilities is the Markov representation. Our design starts off from the *Gilbert Model* [15] in Figure 7, a famous channel model based on two state Markov chain. In the model,  $S$  indicates error-free state, while  $F$  is when the channel is erroneous. The state transition probabilities are denoted as  $p$  and  $q$ . That is, by letting  $Pr(F^n)$  and  $Pr(S^{n-1})$  denote the probabilities of being at states  $F$  and  $S$  at times  $t_n$  and  $t_{n-1}$  respectively, then  $p = Pr(S^n|F^{n-1})$ . Similarly,  $q = Pr(F^n|S^{n-1})$ . Moreover, steady state probabilities of the two states are computed as

$$\pi_S = \frac{p}{p+q}, \pi_F = \frac{q}{p+q} \quad (1)$$

where they indicate the chance of being at the corresponding state at an arbitrary time instant regardless of the initial state, after a sufficient number of state transitions. We follow this model to represent status of a single link. That is, a transmission over the link succeeds if and only if the link is in state  $S$ , while fails in state  $F$ . This lets transition probabilities,  $p$  and  $q$ , to indicate temporal correlation within the link. Extending the model to capture spatiotemporal correlation will be discussed later in Section 4.

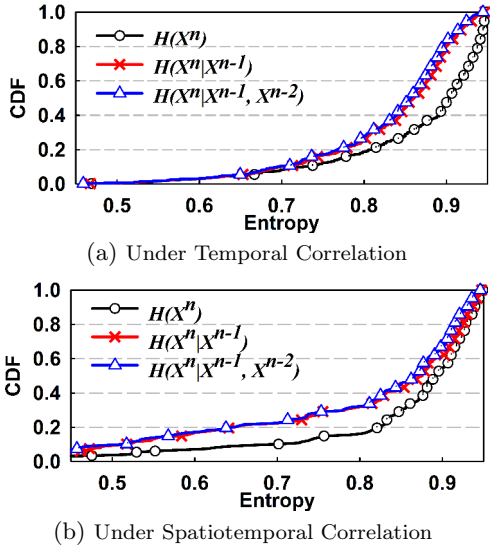


Figure 8: Residual entropies in both (a) and (b) suggest that estimation on correlated links can benefit from 1<sup>st</sup> order Markov chain design, while a higher order model is not necessary.

### 3.2 Validity of 1st Order Markov Design

Our design is based on the Gilbert Model which is a first-order Markov model. In other words, the design benefits from the success/failure information obtained from the previous transmission to infer success of the following transmission. This raises a natural follow-up question: Can we even better estimate the success/failure of the next transmission, given the information on the last two, or even three transmissions? In other words, will a higher order Markov model help to further improve the quality of estimation? To this end, we analyze experimental data to show that the first order Markov model is the right choice; adopting higher order models will not make noticeable differences, while imposing additional complexity to the design and computation.

We achieve this by applying the concept of *entropy* from the information theory, which quantifies the uncertainty within a random variable as number of bits. Higher bit indicates higher uncertainty, which leads to lower estimation quality. Let  $X^n$  be a bernoulli random variable indicating reception success or failure at an arbitrary time instant,  $t_n$ . Then, the entropy within  $X^n$  is denoted as  $H(X^n)$ , indicating the marginal entropy. We further let  $X^{n-1}$  and  $X^{n-2}$  indicate reception success or failure at  $t_{n-1}$  and  $t_{n-2}$ , respectively (i.e., one and two time instants preceding  $X^n$ ). Then, the conditional entropy expresses the amount of uncertainty in  $X^n$  when the value of  $X^{n-1}$  or both  $X^{n-1}$  and  $X^{n-2}$  are known, denoted as  $H(X^n|X^{n-1})$  and  $H(X^n|X^{n-1}, X^{n-2})$ . For brevity entropy computations are given in Appendix A.

Since success or failure can be expressed in a single bit, the maximum uncertainty is 1, when we do not have any clue on success or failure. Conversely, the uncertainty of 0 is when it can be perfectly estimated. Figure 8 shows marginal and conditional entropies in the face of two correlations. Figure 8(a) was obtained from experimental data of  $5 \times 10^5$  consecutive packets over 50 links with packet interval of 6ms, where experiment in Figure 8(b) was done similarly to that in Section 2.1. While achieving the entropy of 0 is impossible due to natural randomness in links caused by shadowing and multipath fading, two clear observations

can be made from the figures: (i) The gaps between conditional and marginal entropies indicate that the knowledge on previous transmission is helpful in estimating the success or failure of the following transmission, again verifying the existence of spatiotemporal and temporal correlations. (ii)  $H(X^n|X^{n-1})$  and  $H(X^n|X^{n-1}, X^{n-2})$  are very close in both figures, suggesting 1st order is as good as higher order design in the estimation quality, despite its lower complexity. This supports the effectiveness and sufficiency of our 1st order Markov-based design.

## 4. MAIN DESIGN

Based on the observations in the previous section we design cETX on top of the Gilbert Model. However, this model is only capable of representing the status of a single link. This means that the model is not enough to express spatiotemporal correlation, which is a relationship across multiple links. In this section, we address this issue by proposing an extended model, from which our metric cETX is derived.

### 4.1 Design Overview

As an extension of ETX, cETX inherits the main idea of ETX to represent link quality by the expected number of transmissions. It is shown later in this section that cETX also retains the additive property of ETX, such that the path cost is simply the sum of cETX. Nevertheless, unlike ETX which assumes the packet receptions are independent, we take both temporal and spatiotemporal correlations into account to more accurately estimate the link/path cost. In fact, cETX is a generalized version of ETX, extended to incorporate knowledge on any degree of correlation into the link/path cost. For example, cETX simply reduces to ETX when there is no correlation among links.

### 4.2 Extended Gilbert Model

We propose an extended representation of the Gilbert Model for a few distinctive features that the original model does not possess. Specifically, it enables (i) the straightforward model extension to multi-hop scenarios, (ii) tracking the packet forwarding status to allow the computation of cETX directly from the model, and (iii) capturing spatiotemporal correlation among consecutive links in a path.

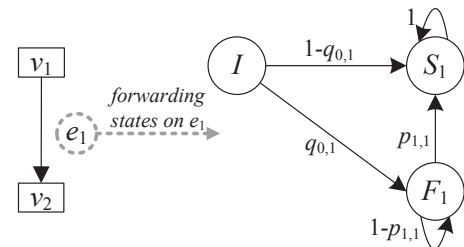


Figure 9: A single-hop network (left) and the corresponding extended Gilbert Model representation (right). The model enables direct computation of our metric as well as straight-forward adaption to multi-hop scenario.

The Extended Gilbert Model describes the forwarding status of each packet in the form of 1<sup>st</sup> order Markov chain. For ease of understanding we start from a single-hop network and its corresponding model depicted in Figure 9. The three states,  $S_1$ ,  $F_1$ , and  $I$ , express packet forwarding on  $e_1$ . States  $S_1$  and  $F_1$  indicate the success and failure of the

transmission over  $e_1$ , while  $I$  stands for the initial state indicating that the transmission has not yet taken place. Then, the packet forwarding process on the model follows intuitive steps: starting from state  $I$ , a transition to either  $S_1$  or  $F_1$  occurs depending on the transmission success or failure. Upon failures, retransmission attempts are made to transit from  $F_1$  to  $S_1$ , until  $S_1$  is reached.

From the definition of state  $I$ , it is clear that its initial probability is 1. Now let us describe the transition probability introduced in the model. Keeping notations consistent to the previous sections, let  $S_1^n$  and  $F_1^{n-1}$  denote the transmission success and failure over  $e_1$  at time  $t_n$  and  $t_{n-1}$ , respectively. Then,  $p_{1,1}$  denotes the probability of a successful transmission after a failure in the previous time instant,  $p_{1,1} = Pr(S_1^n | F_1^{n-1})$ . Note that the subscript  $1,1$  used in  $p_{1,1}$  denotes these two transmissions occur on the same link,  $e_1$ . Essentially  $p_{1,1}$  represents the temporal correlation between consecutive transmissions within  $e_1$ . On the contrary,  $q_{0,1}$  simply indicates the probability of failure in the initial transmission over  $e_1$ . Zero in the subscript implies that no previous transmission exists. Because we do not retransmit a packet that has already been received, the transition probability from  $S_1$  to any other state is 0. In other words, the forwarding process over link  $e_1$  terminates once  $S_1$  has been reached.

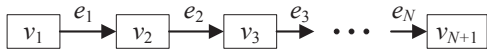


Figure 10: N-hop Linear Network

### 4.3 Multi-hop Gilbert Model

In the previous section we proposed the extended Gilbert Model for a single-hop network. We now further expand the model to a multi-hop scenario depicted in Figure 10.

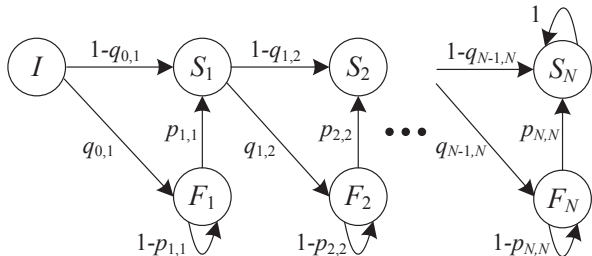


Figure 11: N-hop Gilbert Model

The multi-hop Gilbert Model for the corresponding network is given in Figure 11, where it is an extension from the model in Figure 9 to express multiple links. As shown in the figure, the extension is as simple as adding a pair of  $S$  and  $F$  states per link. Then, the spatiotemporal parameter is introduced between consecutive links. In the multi-hop path once a successful transmission takes place in the preceding link, an immediate transmission follows in the next link. For instance,  $v_2$  starts its transmission over  $e_2$  shortly after the transmission success from  $v_1$  to  $v_2$  over  $e_1$ . The dependency between these two consecutive events is spatiotemporal correlation, which can be represented as  $q_{1,2} = Pr(F_2^n | S_1^{n-1})$  where the subscript  $1,2$  on  $q_{1,2}$  denotes that success at previous time  $t_{n-1}$  occurred on  $e_1$ , where the following failure was on  $e_2$ . Generally, spatiotemporal dependency is considered between any two consecutive links, indicated as  $q_{i-1,i}$  for  $2 \leq i \leq N$  in the multi-hop Gilbert Model. Clearly the multi-hop model captures both temporal and spatiotemporal correlation via  $p$  and  $q$  parameters.

### 4.4 cETX Computation

We now show how our metric cETX can be computed from the multi-hop model in Figure 11. Note that cETX over a link is defined as the estimated number of transmissions to deliver a packet over the link. Suppose we want to compute cETX for an arbitrary link,  $cETX_{e_i}$ . Transmission on  $e_i$  starts on state  $S_{i-1}$ , and ends when  $S_i$  has been reached ( $I$  and  $S_1$  for  $e_1$ ). Since the state transition occurs for every transmission, the  $cETX_{e_i}$  value equals the expected number of transitions to reach state  $S_i$  from  $S_{i-1}$ . This is often referred to as the expected first passage time in Markov chain theory, which can be computed as follows:

$$cETX_{e_i} = 1 + q_{i-1,i} \times \frac{1}{p_{i,i}} \quad (2)$$

The equation can be intuitively understood by referring to our model. The first term in Eq.(2), i.e., 1, indicates the initial transmission which is mandatory. The second term indicates the product of the initial transmission failure probability, i.e.,  $q_{i-1,i}$ , and the expected number of transmissions under the failure of the initial transmission, i.e.,  $\frac{1}{p_{i,i}}$ . Therefore, the equation simply implies that a low cETX value is achievable where there are two conditions: (i) a small chance of the failure in the initial transmission, and (ii) a high chance of recovering from the failure in case the initial transmission fails.

**Special Case:** Eq.(2) shows that cETX is a function of spatiotemporal ( $q_{i-1,i}$ ) and temporal ( $p_{i,i}$ ) correlation parameters. However, the initial link  $e_1$  is a special case as there is no link preceding it. In other words,  $e_1$  has no link to be spatiotemporally correlated to it. Therefore  $q_{0,1}$  is expressed solely in terms of temporal correlation parameters,  $p_{1,1}$  and  $q_{1,1}$ , to be the steady state probability of  $F_1$ . Please note that  $q_{1,1}$  is found in the original Gilbert Model ( $q$  in Figure 7). Borrowing the steady state probability in Eq.(1) and rewriting with our notations, we have

$$q_{0,1} = \frac{q_{1,1}}{p_{1,1} + q_{1,1}} \quad (3)$$

The rationale behind this equation is as follows. The first transmission on the initial link is triggered at an arbitrary time instant, whenever the sender has a packet to transmit. This indicates that we need to estimate the link state at time  $t_n$  without the knowledge of the state at  $t_{n-1}$ . In this case, our best estimate becomes the steady state probability of  $S_1$ , which is simply the ratio of the time  $e_1$  spent in  $S_1$ . Now, we can finally obtain  $cETX_{e_1}$  by plugging in Eq.(3) to Eq.(2).

$$cETX_{e_1} = 1 + \frac{q_{1,1}}{(p_{1,1} + q_{1,1}) \cdot p_{1,1}} \quad (4)$$

**Path cETX:** Our metric retains the additive property of ETX, indicating that path cETX is the sum of link cETXs in the path. This serves as the key that allows us to find the optimal path with cETX with appropriate modifications to traditional shortest path algorithms, which will be discussed in later part of the paper. For a proof on the additive property, let us again consider the network and its model in Figures 10 and 11, where  $cETX_E$  represents the cETX of the entire  $N$ -hop path. Then,  $cETX_E$  is the expected first passage time from state  $I$  to  $S_N$ . Let the first passage time from state  $I$  to  $S_1$  be denoted by a random variable  $Y_1$ , from  $S_1$  to  $S_2$  as  $Y_2$ , and so on until  $Y_N$ . Then, by defini-



tion  $cETX_E$  is the expected value of the sum of all  $Y_i$ , i.e.,  $cETX_E = E[\sum_{i=1}^N Y_i]$ . Due to the linearity of expectation and since  $cETX_{e_i} = E[Y_i]$ , we have

$$cETX_E = \sum_{i=1}^n cETX_{e_i} \quad (5)$$

Hence the additive property holds. We also note that cETX is indeed a generalized version of ETX, and it simply reduces to ETX under independent packet receptions. Proof on the relationship between cETX and ETX under different degrees of correlations is given in Appendix B.

## 5. IMPLEMENTATION ISSUES

This section describes how to obtain the parameters  $p$  and  $q$  for cETX computation, and shows *burst probing* enables precisely measuring the true performances of wireless links.

$e_1$	F	F	S	F	S	F	F	S	S	F	F	S
$e_2$	F	F	F	F	S	F	F	S	S	S	S	S
	$t_0$	$t_1$	$t_2$	$t_3$	$t_4$	$t_5$	$t_6$	$t_7$	$t_8$	$t_9$	$t_{10}$	$t_{11}$

Figure 12: Parameter Computation Example

### 5.1 Parameter Computation

Among the parameters required by our design, those related to temporal correlation within a link are  $p$  and  $q$ . We again use  $S_n$  and  $F_n$  to denote the transmission success and failure at  $t_n$ . Let us compute the  $p$  and  $q$  values for  $e_2$  in Figure 12. Maximum likely estimation for these parameters can be obtained simply by counting the number of transitions between success and failure, which turns out to be  $p_{2,2} = Pr(S_2^n | F_2^{n-1}) = 1/3$  and  $q_{2,2} = Pr(F_2^n | S_2^{n-1}) = 1/5$  for  $0 < n \leq 11$ . Similarly, the spatiotemporal correlation parameter when  $e_1$  precedes  $e_2$  is also computed as  $q_{1,2} = Pr(F_2^n | S_1^{n-1}) = 1/2$ .

### 5.2 Measurement in Practice

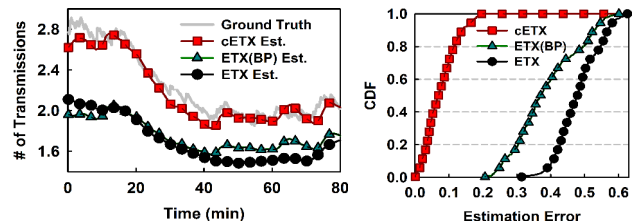
Probing refers to the technique of transmitting a small number of packets to support some fundamental functions including link quality measurement and neighbor discovery. Thus probes are commonly utilized in various state-of-the-art link metrics [10, 14, 25, 26]. Specifically, they adopt the classical periodic probing, where a single probe message is broadcast every fixed interval. However this mechanism suffers from limitations in measuring link performances; We observe that immediate retransmissions and relays induce a stream of packets within a short time interval to impose correlations between transmissions, which cannot be captured by periodic probes. To address this issue, we propose burst probing, where a batch of consecutive probes are sent at a short time interval. In the meantime, to keep the overhead at a reasonable level, the interval between probe bursts is set such that the number of probe packets per unit time is kept the same as that of periodic probing. This ensures the equivalent amount of overhead when cETX replaces ETX.

Unlike temporal parameters, measuring the spatiotemporal parameter via probing incurs additional overhead. This is because the spatiotemporal parameter for a link needs to be measured for every preceding link. To avoid such overhead, we obtain spatiotemporal parameters via the normal data traffic. Recall that the spatiotemporal correlation parameter is simply the failing probability of the initial trans-

mission, just after the packet is received from the preceding link. This statistic can be easily collected; whenever a node receives a data packet, it records the preceding link, as well as the transmission success/failure of the initial transmission. This information is piggybacked on probes to be broadcast to its neighbors. To sum up, cETX assumes spatiotemporal independence under data traffic volume insufficient to obtain spatiotemporal parameter, where the accuracy of cETX nevertheless exceeds that of ETX due to the consideration of temporal correlation. Spatiotemporal correlation is reflected as the traffic increases, where multiple data flows in the network offer cETX with more opportunity to select better routes considering spatiotemporal correlation.

### 5.3 Overhead under Link Dynamics

We run an experiment to compare the link estimation performances of cETX and ETX in relation to the overhead they induce. To summarize, our result indicates estimation error for cETX is only 1/3 of ETX, at the cost of only 0.7% additional overhead. Experimental details are as follows: Burst probing in cETX occurs every 40s, where five consecutive probes are sent each time. ETX sends one probe every 8s. Both probing schemes induce overhead of 1/8 probe per second, indicating a fair comparison. To further maintain fairness, both metrics use the history of up to 90 probes, the value suggested by ETX [11]. In other words, when there is a data packet to be forwarded (every 10s in our case), both metrics use the history of the last 90 probes to estimate the number of (re)transmissions until a successful delivery. Then, the estimations are compared to the number of transmissions that actually occurs, to verify their accuracies. The 80-minute experiment consists of 11 MICAz nodes,  $v_1$  through  $v_{11}$ . One node ( $v_1$ ) serves as the sender while all others are receivers.



(a) Estimation under dynamics (b) Error distribution

Figure 13: Link estimation with cETX closely reflects the actual value (i.e., the ground truth) while ETX is rather optimistic. This is because cETX accounts for bursty losses which ETX fails to capture.

Figure 13(a) shows the result on a link between  $v_1$  and  $v_8$ . The ground truth indicates the actual number of transmissions, while other curves are estimations based on probe history. Furthermore, Figure 13(b) exhibits the distribution of the estimation error (i.e., the absolute difference from the ground truth). We note that there are two versions of ETX in the figure, where one is the original ETX with periodic probing and the other is the modified ETX with burst probing. From the figures, we find that the estimate of cETX is far better than both versions of ETX. The average estimation error of cETX, ETX with burst probing, and original ETX in all ten links are 0.16, 0.42, and 0.48. The performance of ETX with burst probing sits in between cETX and the original ETX because it benefits from burst probing which mimics the data (re)transmission scenario, but it

fails to accurately capture the correlation within. We note that the degree of cETX’s advantage in accuracy applies to the link metrics built on top of ETX, such as 4B [14].

The overhead incurred by probes is approximately 3.2% of the total energy consumed. Since probing is adopted in the majority of the link metrics, its overhead should be amortized. On the other hand, exclusive overhead introduced by our design is the extra information piggybacked on probe packets. This takes up a tiny portion of about 0.7% of the total energy consumption.

## 5.4 Compatibility with Different MAC

The generality of cETX allows it to be applied to networks running various MAC protocols. This is because (i) both contention-based [9, 29, 43] and reservation-based [31, 44] MACs adopt a quick-retransmission policy for lost packet, which incurs temporally correlated, consecutive loss captured by cETX. For example CSMA commonly serves as the basis function for contention-based MACs, where the retransmission for a lost packet is made after a short duration of ACK timeout – 864us and 372us for ZigBee [39] and Wi-Fi [38], respectively. (ii) Spatiotemporal correlation captured via data traffic in cETX naturally reflects the forwarding scheme adopted by the network. That is, the corresponding degree of spatiotemporal correlation is captured regardless of immediate or delayed (e.g., duty cycled networks) packet forwarding. Immediate forwarding is likely to exhibit spatiotemporal correlation. On the other hand, when the delay is sufficiently large, cETX reflects the independence between consecutive links (i.e., no spatiotemporal correlation) where cETX still remains more accurate than ETX due to its consideration on temporal correlation.

## 6. UNICAST/BROADCAST OVER CETX

Replacing the popular metric of ETX, cETX can be generically applied to many protocols. This section presents how optimality is maintained in unicast protocols, followed by the benefit to broadcast schemes.

### 6.1 Application to Unicast

When spatiotemporal correlation is considered, the cETX value of a link is dependent on the preceding link. In this section we demonstrate via an example, how optimal shortest path can be found in a distributed manner using distance vector with two-hop information.

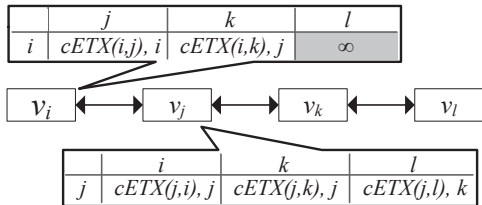


Figure 14: cETX in Unicast – Example Scenario

Let us consider a simple four-node network in Figure 14, where  $cETX(i, j)$  indicates cETX from node  $v_i$  to  $v_j$ . Initially, nodes attain local information about their two-hop neighbors by exchanging information between one-hop neighbors. Then the problem becomes: How cETX beyond two hops can be obtained through further iterative exchanges. That is, how the gray box in  $v_i$ ’s distance vector (i.e.,  $cETX(i, l)$ )

can be found. First, we note that  $cETX(i, l) \neq cETX(i, j) + cETX(j, l)$ , as  $cETX(j, l)$  does not reflect the effect of correlation among the link between  $v_i$  and  $v_j$  and the link between  $v_j$  and  $v_k$ . Instead,  $cETX(i, l)$  can be obtained via the below relationship:

$$cETX(i, l) = cETX(i, k) + cETX(j, l) - cETX(j, k)$$

where last the term,  $cETX(j, k)$ , is the cost of link between  $v_j$  and  $v_k$  *not considering* the correlation with the link between  $v_i$  and  $v_j$  (i.e., the special case in Section 4.4). Referring back to Figure 14, the above equation implies that  $v_i$  can obtain  $cETX(i, l)$  via exchange of distance vector with its direct neighbor,  $v_j$ . In fact, the equation can be generally applied to finding cETX to any multiple hops (i.e.,  $v_l$  of any hop distance from  $v_i$ ), given that  $v_j$  and  $v_k$  are one and two-hop neighbors to  $v_i$ .

**The case of convergecast:** Support of unicast, the most fundamental data delivery mechanism, indicates cETX’s applicability to a wide range of protocols whom unicast serves as their basis operation. Convergecast is one example, which consists of unicasts whose destinations are the sink. In convergecast the impact of spatiotemporal correlation is determined by immediate or delayed forwarding, where cETX inherently covers both the cases via its unicast support.

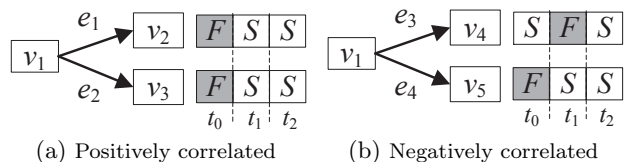


Figure 15: Benefit of cETX in broadcast: (a) and (b) require 1.25 and 1.66 transmissions to deliver 2 packets to both receivers. Performance improves when receivers are positively correlated, which can be captured by cETX.

### 6.2 Application to Broadcast

This section presents how cETX can help improve the performance of broadcast protocols. First, let’s consider the positively correlated case in Figure 15(a). If  $v_1$  starts broadcast at  $t_0$ , the two receivers will both receive the second packet at  $t_1$ , causing two transmissions to deliver the packet to both receivers. If the broadcast starts at  $t_1$ , the two receivers immediately receive the packet, indicating that a single transmission is consumed. Similarly, at  $t_3$ , only one transmission is required. Therefore, an average of  $(2 + 1 + 1)/3 = 1.25$  transmissions are needed for the network in Figure 15(a), while it is  $(2 + 2 + 1)/3 = 1.66$  in Figure 15(b). Here we calculate the expected number of transmissions –  $E(T)$  for a source node to reliably broadcast one packet to all the receivers with the consideration of temporal and spatial correlation using cETX. Without loss of generality, we assume that the link quality of the  $N$  receivers satisfies  $Pr(S_1^n) \geq Pr(S_2^n) \geq \dots \geq Pr(S_N^n)$ . Since the node with a better link receives most of the packets earlier than the node with a worse link [37], we have

$$E(T) = \frac{1}{Pr(S_1^n)} + \sum_{i=2}^N \frac{Pr(F_i^n | S_{i-1}^n)}{Pr(S_i^n)} = \sum_{i=1}^N cETX_{e_i} - N + 1 \quad (6)$$

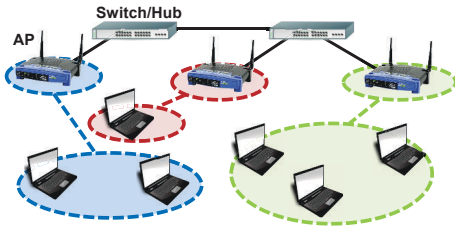


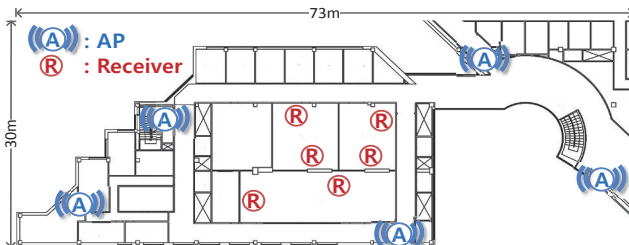
Figure 16: Collaborative broadcast in Wi-Fi. APs connected via wires cooperatively deliver data to all the users (laptops). Dotted circles indicate user groups assigned to APs. In cETX a group consists of highly correlated users.

This lets cETX to be integrated within various broadcast protocols by selecting forwarder which minimizes  $E(T)$ .

Eq.(6) can be further applied to a novel communication paradigm for Wi-Fi networks, demonstrated in Figure 16. In collaborative broadcast multiple APs connected via wires share the same data to collaboratively deliver it to all users. Grouping and assigning users to APs are done via Eq.(6). Both ordinary and collaborative broadcasts are further described and evaluated in the next section.



(a) ZigBee (lab)



(b) Wi-Fi (university building)

Figure 17: ZigBee and Wi-Fi Testbeds

## 7. TESTBED EXPERIMENTATION

In this section we show that our design can be universally applied to various wireless technologies under different scenarios: We evaluate the performance of cETX in indoor testbeds on ZigBee (802.15.4) and Wi-Fi (802.11) platforms, under unicast and broadcast scenarios with twelve protocols.

### 7.1 Baseline

Various representative studies in unicast and broadcast domains are implemented for cETX evaluation.

- **Unicast:** We adopt cETX in three representative unicast routing protocols. (i) **LQSR** [13]: Extends the DSR [20] protocol by taking unreliable links into account. (ii) **sr-cRR** [4]: Similar to LQSR, but without path switching to improve network robustness. (iii) **OLSR** [17]: Routing is executed only through a subset of nodes (i.e., Multi Point

Relays) to reduce the control overhead. The three protocols offer different degrees of freedom in path selection to affect the benefit of cETX.

- **Broadcast:** We integrate cETX to nine classical broadcast protocols with diverse underlying network structures, showing the wide applicability of cETX. (i) **tree based:** C-Tree [7], (ii) **cluster based:** forwarding node cluster (Cluster) [40], (iii) **Multi-Point Relay:** MPR [30], (iv) **pruning based:** Self Pruning (SP [24]), Dominating Pruning (DP [24]), Partial Dominating Pruning (PDP [27]), and Total Dominating Pruning (TDP [27]), (v) **RNG based:** RNG relay subset (RNG [18]), and finally, (vi) **network coding based broadcast protocols:** CODEB [23].

### 7.2 Performance Metrics

The following performance metrics are adopted through our evaluation.

- **Number of Transmissions:** The average number of (re)transmissions to deliver one packet to the destination. Less number of transmissions indicate energy savings.
- **End-to-End Delivery Delay:** The average latency for a packet to be delivered to the destination.
- **End-to-End Delivery Ratio:** The success probability of a packet delivered end-to-end. That is, the number of (re)transmissions in each link in a path do not exceed the retransmission limit.

### 7.3 Experiment Setup

Experimental results in this section are obtained from two physical testbeds, ZigBee and Wi-Fi, with below settings.

- **ZigBee:** We randomly deploy 22 MICAz motes running TinyOS as shown in Figure 17(a). Transmission power is set to be -25dBm to ensure multi-hop network, up to 5 hops. Node placement is kept the same for all evaluated metrics for fairness. Experiment for each metric lasts for two hours, during which an end-to-end packet delivery is made every four seconds, for a total of 1,800 deliveries per metric. CSMA is performed for each (re)transmission with random delay, where the average interval between retransmissions is approximately 6ms. We limit the maximum number of retransmissions for each packet to be 7 (unless otherwise stated) following most practical systems to safeguard networks from being overwhelmed by retransmissions and collisions. Lastly, time stamps and sequence numbers of the delivered packets are logged in the nodes' flash, and uploaded to a PC at the end of the experiment.

- **Wi-Fi:** Depicted in Figure 17(b), five APs are installed in the corners of the floor, where we use laptops with the Lorcon2 packet injection library [2] to play the role of AP generating downstream traffic. It is a reasonable approach since laptops/PCs are frequently used as APs in practice via software AP [1]. Six receivers are placed in three different rooms, separated by concrete walls. Although mainly 802.11g on channel 6 is used for its popularity, analyses later in the section implies a similar benefit in 802.11b and 802.11n as well. A total of  $10^5$  packet transmissions are made in 40 minutes, with the power of 20dBm. Links with packet reception ratios from 10% to 95% are observed, where we commonly apply EWMA (Exponential Weighted Moving Average) on every metric. Control overhead of different probing (i.e., burst probing in cETX and ETX(BP), and periodic probing in ETX) is kept consistent for fairness.



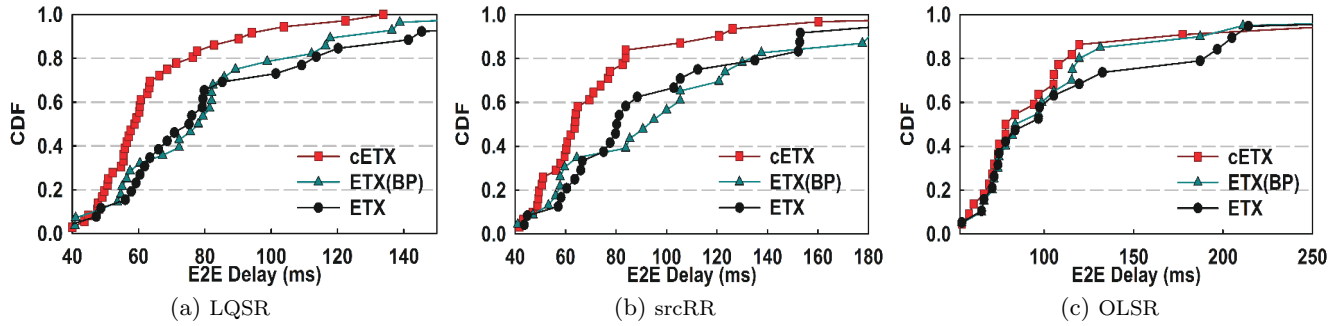


Figure 19: End-to-End Delay: cETX reduces the delay from 10.7% to 26.7% compared to ETX, where the improvement is achieved by the wiser route selection. LQSR allows the highest degree of freedom in the path selection, thus benefits most from cETX.

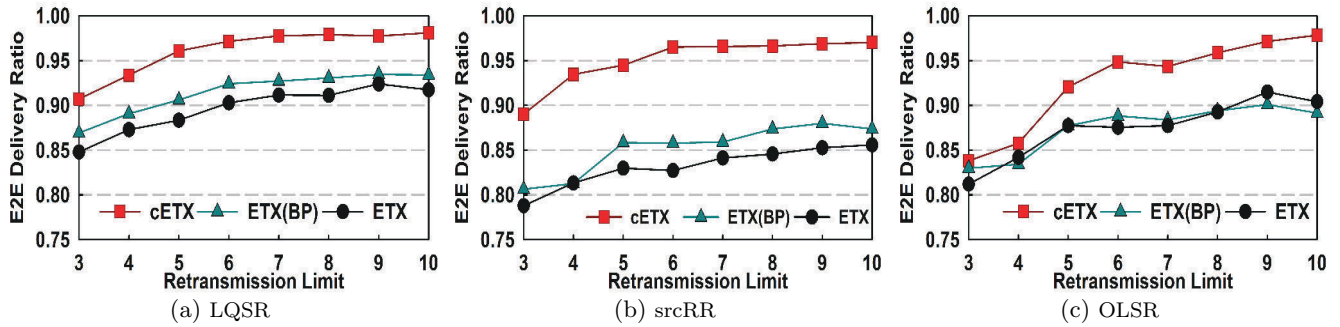


Figure 20: End-to-End Delivery Ratio: cETX tends to select links without burst failures, that are safer from exceeding the retransmission limit. This naturally leads to a higher delivery ratio compared to ETX.

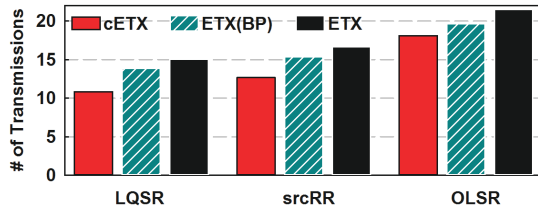


Figure 18: cETX saves 27.8%, 24.1%, and 15.8% of transmissions for LQSR, srcRR, and OLSR, compared to ETX.

## 7.4 Unicast

Figure 18 depicts the performance of cETX on unicast, obtained from the ZigBee testbed in Figure 17(a). Compared to ETX, cETX saves 27.8%, 24.1%, and 15.8% of transmissions for LQSR, srcRR, and OLSR. This demonstrates that cETX makes wiser routing decisions than ETX. Compared to ETX(BP), the percentage of savings becomes 21.6%, 17.5%, and 7.7%. This is because ETX(BP) benefits from burst probing for a slight performance enhancement over the original ETX. Furthermore, the advantage of cETX is the largest for LQSR and smallest for OLSR. The reason for this lies in the number of paths to choose from. While LQSR grants the most freedom in selecting paths, srcRR and OLSR restrict the frequent path switch to avoid high control overhead. Especially, OLSR only allows paths with MPR (Multi Point Relay) nodes. Figure 19 shows the end-to-end delay of metrics in the three protocols. cETX again exhibits the best performance, where the average reduction in delay ranged from 10.7% to 26.7%. Again LQSR obtains

the biggest performance improvement due to the largest selection of paths.

• **Impact of Retransmission Limit:** Now we vary the limitation in the number of retransmissions from 3 to 10 and investigate its effect on the performance. Packet in delivery is dropped whenever the number of transmissions in a single link exceeds the limit, indicating failure in the end-to-end delivery. Note that exceeding the limit requires a link exhibiting continuous failures, which cETX precisely avoids to select. On the other hand, ETX blindly selects paths without considering this issue, leading to a worse delivery ratio. As shown in Figure 20, regardless of protocol cETX consistently achieves delivery ratios of over 94% for retransmission limit of 7 or higher.

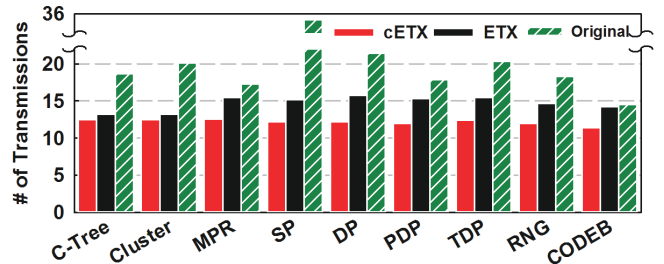
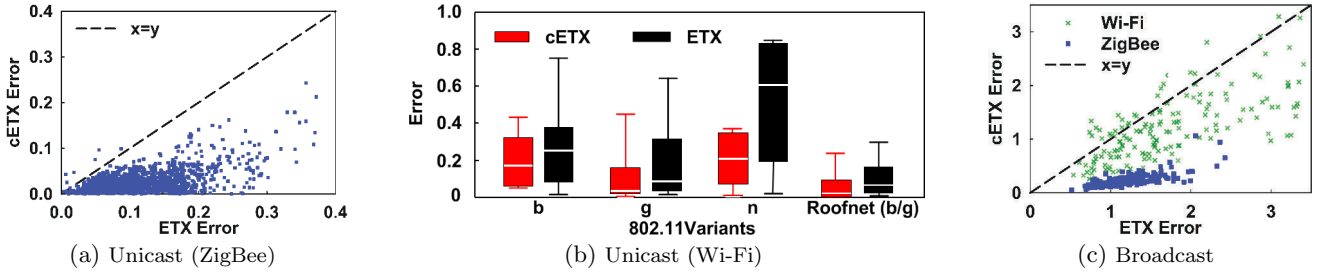


Figure 21: The Performance in Broadcast: cETX saves an average of 37% transmissions in nine broadcast protocols.

## 7.5 Broadcast

The experimental results on nine classical reliable broadcast protocols, tested on ZigBee testbed, are shown in Fig-



**Figure 22: Interpretation error is notably lower in cETX. In unicast cETX error is less than half of ETX. The performance of ETX rapidly drops in 802.11n where the fast transmission rate induces a high temporal correlation among consecutive transmissions. Roofnet shows the smallest error due to the outdoor environment with low degree of wireless interference. Under broadcast cETX reduces the error by 72.3% and 21.5% on ZigBee and Wi-Fi, respectively.**

ure 21. On average, the protocols need 20.5 transmissions to guarantee delivery of a packet to the entire network, while the number becomes 14.7 and 12.2 for ETX and cETX. Knowing that CODEB saves 31.6% of transmissions compared to the schemes without network coding, our design makes a further 21.4% improvement upon CODEB due to following reasons: a low link correlation may cause the nodes in a cluster to lose different packets, causing more retransmissions. With the consideration on spatial and temporal correlations, the protocols benefit from cETX to select forwarders with the minimum transmission cost (i.e.,  $\min(\frac{E(T)}{N})$ ), thus forming clusters with high correlations.

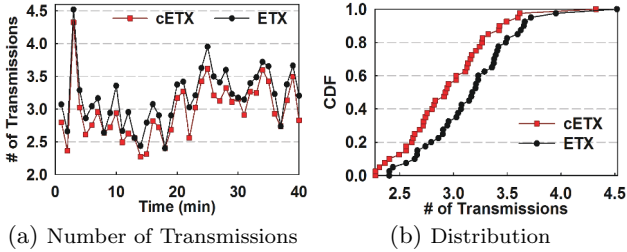


**Figure 23: In (a) cETX consistently reduces number of broadcasts compared to ETX, indicating energy savings. This is shown as distribution in (b).**

Figure 23 shows the improvement achieved for collaborative broadcast on Wi-Fi testbed depicted in Figure 17(b). Five APs collaboratively deliver  $10^5$  packets to all six receivers. As cETX allows grouping highly correlated receivers to minimize retransmissions, its transmission cost is consistently less than or equal to that of ETX. The reduction can be as large as 34.1%.

## 7.6 Performance Insights

This section provides analysis on *why* cETX performs better than ETX. Results on ZigBee platform are obtained from the 11-node experiment in Section 5.3. For Wi-Fi, experiments with six receivers and  $2 \times 10^5$  packets are analyzed for each 802.11 variant: b, g, and n. We also analyze large-scale public Wi-Fi traces ( $5.6 \times 10^5$  packets from 560 links) from the MIT’s Roofnet project [3] to validate the generality of our design.

**• Interpretation accuracy in unicast:** We first show the metrics’ abilities to accurately interpret the probe reception history. That is, given the history, we observe how precisely a metric captures the performance of the corresponding link. This is done by comparing ETX and cETX values to the true value, introduced in Section 2.2. We use *error* as the

measure of interpretation quality, which is the absolute difference between the metric and the true value. The result on ZigBee platform is depicted in Figure 22(a). Error for cETX is less than that of ETX for most of the time, where it is 70.2% less on average. This is because ETX fails to capture highly correlated burst failures. This trend continues to Wi-Fi in Figure 22(b) regardless of its variants; ETX errors exceed those of cETX by 45.1%, 84.7%, and 160.3% in 802.11b, g, and n. Analysis on the Roofnet trace, which is a mixture of 802.11b and g, indicate the error is 49.6% larger in ETX. We note that error in Roofnet trace is generally smaller compared to our experiments; Roofnet is measured in outdoor deployment, where the degree of interference (i.e., the main cause of burst failures) is limited.

**• Interpretation accuracy in broadcast:** In both traditional and collaborative broadcasts, multiple receivers form a cluster in which members receive the packets from the designated sender. (i.e., APs) A smart grouping of receivers and assigning them with the right sender play a key role in determining the efficiency of the network. With the consideration of link correlation, cETX shows an improved accuracy compared to ETX in computing the expected number of transmissions required for a cluster for a given sender, as presented in Figure 22(c). Similarly to the unicast case, error is defined to be the absolute value of the difference of the true value and the values computed by cETX and ETX. The figure shows adopting cETX reduces the error by up to 67.6% in Wi-Fi where in ZigBee it is as high as 91.4%. This is because multiple low-power ZigBee links can easily be victims of cross-network interferences, inducing correlation among links. On average, cETX reduces the error by 21.5% and 75.3% in Wi-Fi and ZigBee, respectively. This advantage provides a rational explanation of the transmission (i.e., energy) saving achieved in the broadcast protocols shown earlier in the section.

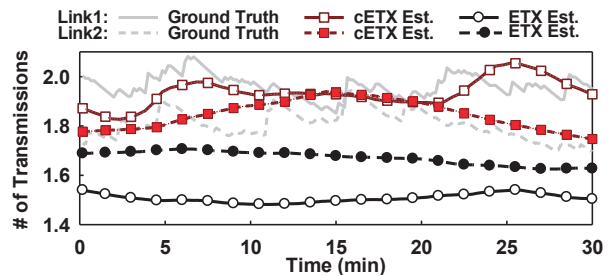


**Figure 24: Unlike ETX, cETX accurately estimates the ground truth, where the quality of Link2 is either better or at least similar to that of Link1.**

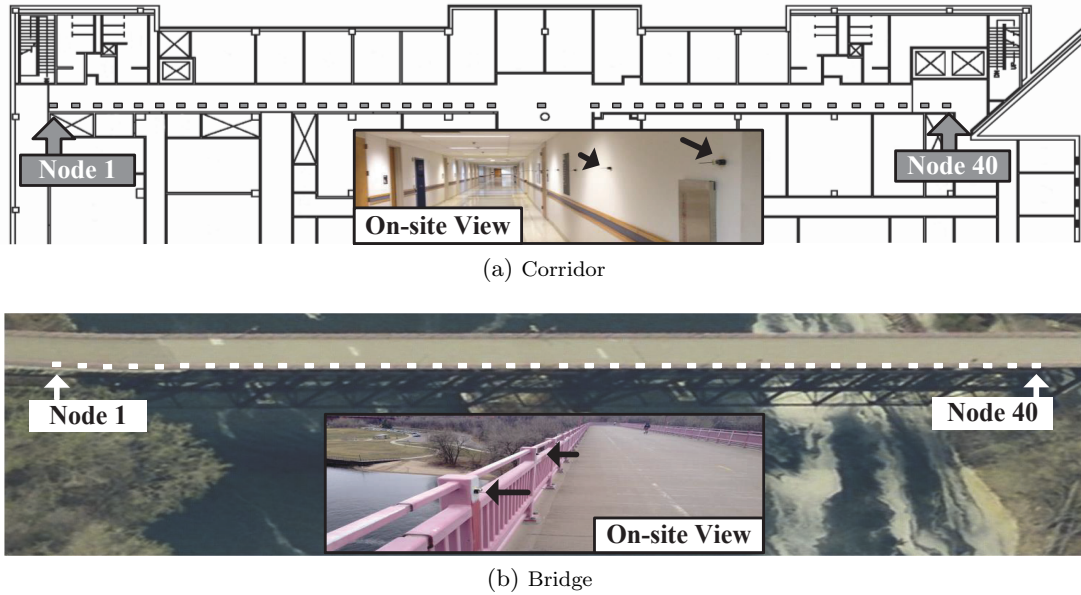


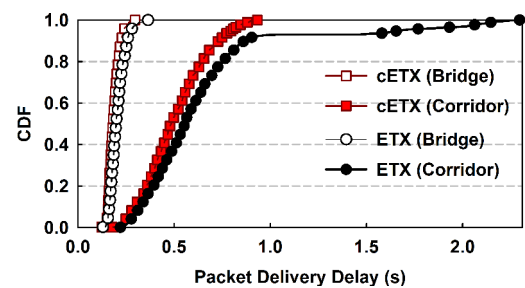
**Figure 25: Indoor (corridor) and outdoor (bridge) experiment setup.** On each site 40 MICAz nodes are linearly deployed every 1.8m, for 70m. In the corridor nodes were attached to the wall, 1.8m above the floor, while on the bridge they were deployed on the steel fence of height 1.5m. The corridor is within a university building with heavy Wi-Fi traffic.

•**Estimation accuracy and route selection:** An inaccurate interpretation leads to an imprecise link quality estimation and further, a sub-optimal route selection. We show how this occurs in practice via Figure 24, showing the estimated and real number of transmissions on two distinct links for 30 minutes. The figure conveys two ideas: (i) cETX estimation is more precise and thus (ii) cETX makes better routing decision. When making a selection between links 1 and 2, ETX suggests link 1 should be chosen over link 2, due to the lower ETX value. However, the ground truth indicates otherwise, i.e., link 2 always has a better or similar (at 17<sup>th</sup> min) performance than link 1. cETX is free from this problem, explaining the performance gain obtained in the unicast and broadcast algorithms in the earlier parts of the section.

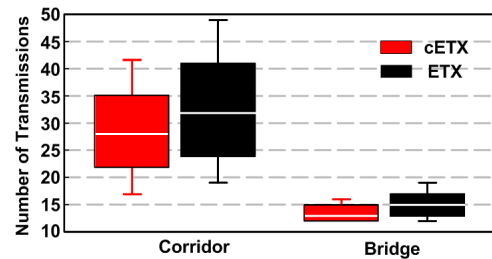
## 8. IN-SITU DEPLOYMENT

In this section we conduct experiments under practical indoor and outdoor settings, in the aim to give a better understanding on the impact of our design in real-world applications. Forty MICAz nodes are deployed in a corridor in a university building and on a bridge crossing a river – common sites for popular applications including tracking and maintenance/safety monitoring – as shown in Figure 25. Nodes are deployed every 1.8m spanning 70m end to end. The transmission power is set to be -15dBm to assure multiple neighbors, where each node roughly has 10-12 neighbors (i.e., 5-6 neighbors to the node’s right and left). Other parameters are kept the same as previous experiments. A thousand end-to-end (i.e., from node 1 to 40) packet deliveries are made, via LQSR embedding either ETX or cETX.

Results on delivery delay, shown in Figure 26(a), suggests that cETX’s performance gain is more significant in the corridor (21.5% reduction) than on the bridge (8.9% reduction). This is due to the degree of wireless interference; In the uni-



(a) Delay distribution



(b) Number of transmissions

**Figure 26: In-situ results for  $10^3$  packet deliveries.**

versity building hundreds of Wi-Fi users are connected to over fifty Wi-Fi access points, creating excessive amount of wireless interference. This causes burst failures in the experiment, forcing ETX to select poorly performing paths suffering from long delivery delays well above 1 second. Similar observation can be made in Figure 26(b). The average number of transmissions are 28.8 and 36.9 for cETX and ETX in the corridor, respectively, indicating 21.9% reduction. Due to the same reason as in the delay case, smaller degree of reduction (9%) is observed on the bridge, compared to what is achieved in the corridor.

## 9. RELATED WORK

Our work is built on top of two phenomena addressed in separate studies, namely, temporal and spatiotemporal correlation. We briefly summarize how the two phenomena have been studied so far in relation to our work.

The impact of temporal correlation in ZigBee network, as well as in Wi-Fi, has been demonstrated clearly via extensive measurements and analyses in [34], where the authors propose a metric to quantify the degree of correlation. Furthermore, the works including BRE [6], 4C [25], and TALENT [26] exploit short-term dynamics based on packet overhearing to utilize intermittent and burst links. In RNP [10] and mETX [22], temporal properties of links were considered in routing, by counting consecutive failures and taking the variance of failure probability, respectively. However, the works in this category pays little or no attention to correlation across different links.

The comprehensive study on packet-level spatial correlation in [33] suggests a metric to predict performances of diversity-based protocols based on the intensity of correlation. To date, the phenomenon has been exploited in a wide range of wireless domains including ZigBee [45], Wi-Fi [33], and cellular networks [26]. For instance, it was utilized in network coding for efficient multicast [21] and broadcast [5]. Furthermore, Spatial correlation was studied in the presence of constructive interference to achieve fast data dissemination [12]. In this work we consider spatiotemporal correlation, which expands the effect of spatial correlation to the time domain. The unified design allows us to improve the unicast performance as well as the broadcast performance. In addition, the previous studies focus on particular protocol designs, while this work provides a generalized form of the widely-adopted ETX. Our work can broadly improve a wide range of protocols.

## 10. CONCLUSION

Our empirical study on temporal and spatiotemporal correlations in packet receptions shed light on the possibility of further improvement in network performance. In this work, we reveal that the most widely adopted link metric, ETX, fails to reflect the true link performance due to the ignorance of correlations. To address this issue, we propose cETX, a generalized version of ETX capturing not only temporal correlation but also spatiotemporal correlation. Because our design keeps the intuitive idea of ETX intact, we can simply replace ETX with cETX in existing protocols to obtain better routing performance. Our evaluations on both ZigBee and Wi-Fi testbeds demonstrate that cETX cuts down the metric error by 75.8% and 62.1%, and saves 22% and 37% communication cost for three unicast and nine broadcast protocols with only 0.7% additional overhead.

## A. ENTROPY COMPUTATION

Introduced in the *information theory*, entropy defines the the amount of uncertainty contained in a random variable. Let  $X^n$  be a bernoulli random variable indicating reception success or failure at time instant  $t_n$ . Then  $H(X^n)$  represents the entropy within  $X^n$ , where it is computed as

$$H(X^n) = - \sum_{x^n \in \{succ, fail\}} Pr(x^n) \log_2 Pr(x^n) \quad (7)$$

which is a marginal entropy as it only considers one random variable, without any given conditions. Furthermore, let  $X^{n-1}$  and  $X^{n-2}$  be bernoulli random variables for reception success or failure at one and two time instants prior to  $X^n$ . Then, the conditional entropy is the degree of uncertainty in  $X^n$ , when the value of  $X^{n-1}$  or both  $X^{n-1}$  and  $X^{n-2}$  are known a priori, denoted as  $H(X^n|X^{n-1})$  and  $H(X^n|X^{n-1}, X^{n-2})$ . The conditional entropies are found by the following equations.

$$\begin{aligned} H(X^n|X^{n-1}) &= H(X^n, X^{n-1}) - H(X^{n-1}) \\ H(X^n|X^{n-1}, X^{n-2}) &= H(X^n, X^{n-1}, X^{n-2}) \\ &\quad - H(X^n|X^{n-1}) - H(X^{n-2}) \end{aligned}$$

where the joint entropies,  $H(X^n, X^{n-1})$  and  $H(X^n, X^{n-1}, X^{n-2})$ , are computed similarly to Eq.(7). That is, by replacing the marginal probability  $Pr(x^n)$  by joint probabilities,  $Pr(x^n, x^{n-1})$  and  $Pr(x^n, x^{n-1}, x^{n-2})$ .

## B. THE PROPERTIES OF CETX

In this appendix we provide the relationship between cETX and ETX, under various degrees of correlations.

• **Under independence:** cETX is a generalized version of ETX, where cETX simply reduces to ETX when packet receptions are independent. For simplicity, we omit the subscript for the following parts of the section. For an arbitrary link, spatiotemporal independence turns *cETX* from Eq.(2) to the form of Eq.(4). Then, when transmissions are temporally independent,

$$Pr(S^n|F^{n-1}) = Pr(S^n|S^{n-1})$$

which leads to  $p + q = 1$ . By plugging in this condition within Eq.(4), we have

$$cETX = \frac{p+q}{p} = \frac{1}{Pr(S^n)} = ETX$$

where we used Eq.(3) and the rationale behind it. Thus, cETX is equivalent to ETX when transmissions are independent.

• **Effect of correlation:** Here we show how cETX is determined in relation to the correlation. For clarity, in direct comparison to ETX, we use cETX in Eq.(4). When link faces failure burst, the following condition holds:

$$Pr(F^n|F^{n-1}) > Pr(F^n|S^{n-1})$$

We thus have  $p + q < 1$ . Plugging in the condition within Eq.(4), we obtain

$$cETX = \frac{q}{(p+q) \cdot p} + 1 > \frac{q}{p} + 1 = ETX$$

Therefore, cETX is larger than ETX when the link experiences burst failure. In other words, ETX normally underestimates the transmission cost because of the ignorance of correlations.

## ACKNOWLEDGEMENT

This work was supported in part by the National Science Foundation under grants CNS-0845994 and CNS-1444021. We sincerely thank our shepherd Dr. Luca Mottola and the reviewers for their valuable comments and feedback.



## 11. REFERENCES

- [1] Hostapd. <http://hostap.epitest.fi/hostapd/>.
- [2] Lorcon wireless packet injection lib. <https://code.google.com/p/lorcon/>.
- [3] Mit roofnet. [http://pdos.csail.mit.edu/roofnet/doku.php?id=publications#sigcomm\\_traces/](http://pdos.csail.mit.edu/roofnet/doku.php?id=publications#sigcomm_traces/).
- [4] D. Aguayo, J. Bicket, and R. Morris. Srcrr: A high throughput routing protocol for 802.11 mesh networks. In *Ph.D. Diss, MIT*, 2004.
- [5] S. M. I. Alam, S. Sultana, Y. C. Hu, and S. Fahmy. Link correlation and network coding in broadcast protocols for wireless sensor networks. In *SECON*, 2012.
- [6] M. H. Alizai, O. Landsiedel, J. A. B. Link, S. Götz, and K. Wehrle. Bursty traffic over bursty links. In *SenSys*, 2009.
- [7] K. Alzoubi, P. Wan, and O. Frieder. New distributed algorithm for connected dominating set in wireless ad hoc networks. In *Hawaii Int. Conf. System Sciences*, 2002.
- [8] R. Banirazi, E. A. Jonckheere, and B. Krishnamachari. Heat-diffusion: Pareto optimal dynamic routing for time-varying wireless networks. In *INFOCOM*, 2014.
- [9] M. Buettner, G. V. Yee, E. Anderson, and R. Han. X-mac: a short preamble mac protocol for duty-cycled wireless sensor networks. In *SenSys*, 2006.
- [10] A. Cerpa, J. L. Wong, M. Potkonjak, and D. Estrin. Temporal properties of low power wireless links: Modeling and implications on multi-hop routing. In *MobiHoc*, 2005.
- [11] D. S. J. De Couto, D. Aguayo, J. Bicket, and R. Morris. A high-throughput path metric for multi-hop wireless routing. In *MobiCom*, 2003.
- [12] M. Doddavenkatappa, M. C. Chan, and B. Leong. Splash: Fast data dissemination with constructive interference in wireless sensor networks. In *nsdi*, 2013.
- [13] R. Draves, J. Padhye, and B. Zill. Routing in multi-radio, multi-hop wireless mesh networks. In *MobiCom*, 2004.
- [14] R. Fonseca, O. Gnawali, K. Jamieson, and P. Levis. Four-bit wireless link estimation. In *HotNets*, 2007.
- [15] E. N. Gilbert. Capacity of a burst-noise channel. *Bell System Technical Journal*, 39(2), 1960.
- [16] P. Guo, J. Cao, K. Zhang, and X. Liu. Enhancing zigbee throughput under wifi interference using real-time adaptive coding. In *INFOCOM*, 2014.
- [17] P. Jacquet, P. Muhlethaler, T. Clausen, A. Laouiti, A. Qayyum, and L. Viennot. Optimized link state routing protocol for ad hoc networks. In *IEEE INMIC*, 2001.
- [18] J. Cartigny, F. Ingelrest, and D. Simplot. Rng relay subset flooding protocols in mobile ad hoc networks. *International Journal of Foundations of Computer Science*, 2003.
- [19] S. Ji, R. Beyah, and Z. Cai. Snapshot/continuous data collection capacity for large-scale probabilistic wireless sensor networks. In *Infocom*, 2012.
- [20] D. B. Johnson and D. A. Maltz. Dynamic source routing in ad hoc wireless networks. In *Mobile Computing*, 1996.
- [21] A. Khreishah, I. M. Khalil, and J. Wu. Distributed network coding-based opportunistic routing for multicast. In *MobiHoc*, 2012.
- [22] C. E. Koksal and H. Balakrishnan. Quality-aware routing metrics for time-varying wireless mesh networks. *IEEE Journal on Selected Areas in Communications*, 24(11), 2006.
- [23] E. L. Li, R. Ramjee, M. M. Buddhikot, and S. C. Miller. Network coding-based broadcast in mobile ad-hoc networks. In *INFOCOM*, 2007.
- [24] H. Lim and C. Kim. Flooding in wireless ad hoc networks. In *Computer Communications Journal*, 2001.
- [25] T. Liu and A. Cerpa. Foresee (4c): Wireless link prediction using link features. In *IPSN*, 2011.
- [26] T. Liu and A. Cerpa. Talent: Temporal adaptive link estimator with no training. In *SenSys*, 2012.
- [27] W. Lou and J. Wu. On reducing broadcast redundancy in ad hoc wireless networks. *IEEE Transactions on Mobile Computing*, 2002.
- [28] S. Patten, B. Krishnamachari, and R. Govindan. The impact of spatial correlation on routing with compression in wireless sensor networks. *ACM TOSN*, 2008.
- [29] J. Polastre, J. Hill, and D. Culler. Versatile low power media access for wireless sensor networks. In *SenSys*, 2004.
- [30] A. Qayyum, L. Viennot, and A. Laouiti. Multipoint relaying for flooding broadcast messages in mobile wireless networks. In *HICSS*, 2002.
- [31] I. Rhee, A. Warriar, M. Aia, and J. Min. Z-mac: A hybrid mac for wireless sensor networks. In *SenSys*, 2005.
- [32] K. Srinivasan, P. Dutta, A. Tavakoli, and P. Levis. An empirical study of low-power wireless. *ACM TOSN*, 6(2), 2010.
- [33] K. Srinivasan, M. Jain, J. I. Choi, T. Azim, E. S. Kim, P. Levis, and B. Krishnamachari. The kappa factor: Inferring protocol performance using inter-link reception correlation. In *MobiCom*, 2010.
- [34] K. Srinivasan, M. A. Kazandjieva, S. Agarwal, and P. Levis. The beta-factor: Measuring wireless link burstiness. In *SenSys*, 2008.
- [35] J. Tang, G. Xue, C. Chandler, and W. Zhang. Interference-aware routing in multihop wireless networks using directional antennas. In *INFOCOM*, 2005.
- [36] P.-J. Wan, Z. Wang, H. Du, S. C.-H. Huang, and Z. Wan. First-fit scheduling for beaconing in multihop wireless networks. In *INFOCOM*, 2010.
- [37] S. Wang, S. M. Kim, Y. Liu, G. Tan, and T. He. Corlayer: A transparent link correlation layer for energy efficient broadcast. In *MobiCom*, 2013.
- [38] Wireless LAN Working Group. Ieee standard part 11: Wireless lan medium access control (mac) and physical layer (phy) specifications. *IEEE Std 802.11-2012 (Revision of IEEE Std 802.11-2007)*, pages 1–2793, March 2012.
- [39] Wireless Personal Area Network (WPAN) Working Group. Ieee standard part 15.4: Low-rate wireless personal area networks (lr-wpans). *IEEE Std 802.15.4-2011 (Revision of IEEE Std 802.15.4-2006)*, pages 1–314, Sept 2011.

- [40] J. Wu and W. Lou. Forward-node-set-based broadcast in clustered mobile ad hoc networks. In *Wireless Comm. and Mobile Comp.*, 2003.
- [41] J. Wu, M. Lu, and F. Li. Utility-based opportunistic routing in multi-hop wireless networks. In *ICDCS*, 2008.
- [42] G. Xing, M. Li, H. Luo, and X. Jia. Dynamic multiresolution data dissemination in wireless sensor networks. *IEEE Trans. Mob. Comput.*, 2009.
- [43] W. Ye, J. Heidemann, and D. Estrin. Medium access control with coordinated, adaptive sleeping for wireless sensor networks. *IEEE/ACM Transactions on Networking*, 2003.
- [44] W. Ye, F. Silva, and J. Heidemann. Ultra-low duty cycle mac with scheduled channel polling. In *SenSys*, 2006.
- [45] G. G. J. B. T. G. Zhiwei Zhao, Wei Dong and C. Chen. Modeling link correlation in low-power wireless networks. In *INFOCOM*, 2015.